Climate-Driven Ecosystem Succession in the Sahara: The Past 6000 Years

S. Kröpelin,[1]* D. Verschuren,[2] A.-M. Lézine,[3] H. Eggermont,[2] C. Cocquyt,[2,4] P. Francus,[5,6] J.-P. Cazet,[3] M. Fagot,[2] B. Rumes,[2] J. M. Russell,[7] F. Darius,[1] D. J. Conley,[8] M. Schuster,[9] H. von Suchodoletz,[10,11] D. R. Engstrom[12]

Desiccation of the Sahara since the middle Holocene has eradicated all but a few natural archives recording its transition from a "green Sahara" to the present hyperarid desert. Our continuous 6000-year paleoenvironmental reconstruction from northern Chad shows progressive drying of the regional terrestrial ecosystem in response to weakening insolation forcing of the African monsoon and abrupt hydrological change in the local aquatic ecosystem controlled by site-specific thresholds. Strong reductions in tropical trees and then Sahelian grassland cover allowed large-scale dust mobilization from 4300 calendar years before the present (cal yr B.P.). Today's desert ecosystem and regional wind regime were established around 2700 cal yr B.P. This gradual rather than abrupt termination of the African Humid Period in the eastern Sahara suggests a relatively weak biogeophysical feedback on climate.

One of the most prominent environmental changes of the past 10,000 years is the transition of northern Africa from a "green Sahara" (*1*) during the early Holocene "African Humid Period" (*2*) to the world's largest warm desert today. Detailed knowledge of the tempo and mode of this transition is crucial for understanding the interaction between tropical and mid-latitude weather systems (*3*–*6*) and the multiple impacts of mineral aerosols exported from the Sahara on global climate (*7*–*10*) and distant ecosystems (*11*–*13*). The distinct lack of high-quality paleoenvironmental records covering the past four to five millennia from within the Sahara desert (*14*) (SOM text 1) has directed substantial effort to the modeling of African monsoon dynamics in response to orbital insolation changes (e.g., *15*, *16*), and of the influence of surface temperature changes in the adjacent tropical ocean (e.g., *4*) and biogeophysical feedbacks between climate and vegetation (*1*, *17*–*20*). Modeling results suggest that a strong positive biogeophysical feedback between rainfall and vegetation (*18*) appear to be supported by the record of terrigenous (land-eroded) dust deposited in deep-sea sediments downwind from the Sahara, which shows a sudden increase at 5500 calendar years before the present (cal yr B.P.) (*2*, *21*). As a result, the Holocene drying of the Sahara (i.e., termination of the "African Humid Period") is widely believed to have been an abrupt event, completed within a few hundred years (e.g., *22*, *23*). In turn, this abrupt event of possible continental scale is regarded as a prime example of catastrophic regime shifts in natural ecosystems (e.g., *24*, *25*).

In this context, we present a continuous and accurately dated paleo-environmental record covering the past 6000 years from within the Sahara, using multiple proxies and indicators preserved in a finely laminated lake-sediment sequence from northern Chad. High-resolution sedimentological and geochemical data coupled with biological indicators (pollen, spores, and the remains of aquatic biota) permit a precise reconstruction of terrestrial and aquatic ecosystem response to climate-driven moisture-balance changes in the now hyperarid core of the east-central Sahara desert.

Study site and material. Lake Yoa is one of a handful of permanent lakes occupying Pleistocene deflation basins in Ounianga, situated halfway between the Tibesti and Ennedi mountains (Fig. 1). The subtropical desert climate of this area is characterized by high daytime temperatures, negligible rainfall, and dry northeasterly trade winds blowing almost year-round through the Tibesti-Ennedi corridor (Fig. 1C) (SOM text 2). The Ounianga lakes are maintained against this extremely negative water balance by groundwater inflow from the Nubian Sandstone Aquifer, which was last recharged during the early Holocene (*26*). This stable groundwater input ensured permanence of the aquatic ecosystem throughout the dry late-Holocene period but dampened its hydrological sensitivity to climate. Sediments in Lake Yoa are finely laminated throughout the sampled upper 7.47 m of the sequence (*27*). Sections with annual lamination (varves) (Fig. 2D) show an average sedimentation rate of 1.3 mm per year, in support of the age-depth model constructed from 12 accelerator mass spectrometry radiocarbon dates and the 1964 caesium marker of nuclear bomb testing (*27*) (table S1).

The Lake Yoa record documents dramatic changes through time in three important components of the Saharan paleoenvironment. First, it traces the evolution of the local aquatic ecosystem from a dilute freshwater habitat to the present-day hypersaline oasis. Second, it reveals the establishment of today's terrestrial desert ecosystem as the result of continuous vegetation succession between 5600 and 2700 cal yr B.P. Third, it shows the changing regional wind regime, culminating in establishment of today's almost year-round northeasterly winds around 2700 cal yr B.P.

Evolution of the aquatic ecosystem. The most prominent feature in the recorded history of Lake Yoa is its relatively rapid transition, between 4200 and 3900 cal yr B.P., from a seemingly stable freshwater habitat (surface-water conductivity of 300 to 500 µS/cm) to a true salt lake (>10,000 µS/cm) in which only specialized fauna and flora can survive (Fig. 2A and figs. S2 to S4) (*27*). In reality, the ecology of Lake Yoa evolved continuously during the past 6000 years, in response to changes in water chemistry, nutrient dynamics, and substrate availability driven by changing lake hydrology and water balance (SOM text 3 and 4). In brief, organic matter deposition (Fig. 2C) (SOM text 5) and the stratigraphy of phytoplankton species (figs. S2 and S3) indicate that Lake Yoa switched from a less to a more productive aquatic ecosystem ~5600 cal yr B.P. Lake productivity remained high after the fresh-to-saline transition until ~3300 cal yr B.P., when conductivity rose above 20,000 µS/cm (Fig. 2A), and also the most salt-tolerant freshwater biota disappeared (fig. S4). From that moment on, both primary productivity (percentage organic matter) (Fig. 2C) and secondary productivity (represented by fossil chironomid abundance) (fig. S4) gradually declined, until by 2700 cal yr B.P. they stabilized at ~50 to 70% lower values. This transition coincided with a virtually complete collapse of the Lake Yoa diatom flora [biogenic SiO_2 (Fig. 2B); diatom cell counts (fig. S3)]. This fairly unproductive, hypersaline aquatic ecosystem then acquired its modern-day biology with establishment of the

[1]Africa Research Unit, Institute of Prehistoric Archaeology, University of Cologne, Jennerstraße 8, D-50823 Köln, Germany. [2]Limnology Unit, Department of Biology, Ghent University, K. L. Ledeganckstraat 35, B-9000 Gent, Belgium. [3]Laboratoire des Sciences du Climat et de l'Environnement, CNRS-CEA-UVSQ UMR 1572, L'Orme des Merisiers, F-91191 Gif-Sur-Yvette, France. [4]National Botanic Garden of Belgium, Domein van Bouchout, B-1860 Meise, Belgium. [5]Institut National de la Recherche Scientifique, Centre Eau, Terre et Environnement, 490 Rue de la Couronne, Québec, Québec G1K 9A9, Canada. [6]GEOTOP, Geochemistry and Geodynamics Research Centre, C.P. 8888, Université du Québec à Montréal, Succursale, Centre-Ville, Montréal, Québec H3C 3P8, Canada. [7]Geological Sciences, Brown University, Box 1846, Providence, RI 02912, USA. [8]GeoBiosphere Centre, Department of Geology, Lund University, Sölvegatan 12, SE-22362 Lund, Sweden. [9]Institut International de Paléoprimatologie, Paléontologie Humaine, Evolution et Paléoenvironnements, CNRS UMR 6046, Université de Poitiers, 40 Avenue du Recteur Pineau, F-86022 Poitiers, France. [10]Geoforschungszentrum Potsdam, Telegrafenberg, D-14473 Potsdam, Germany. [11]Lehrstuhl für Geomorphologie, Universität Bayreuth, Universitätsstraße 30, D-95440 Bayreuth, Germany. [12]St. Croix Watershed Research Station, Science Museum of Minnesota, Marine on St. Croix, MN 55047, USA.

*To whom correspondence should be addressed. E-mail: s.kroe@uni-koeln.de

salt-loving hemipteran *Anisops* as the dominant macrozooplankton species ~2700 cal yr B.P. and appearance of brine flies (*Ephydra*) ~1500 cal yr B.P. (fig. S2).

Evolution of the terrestrial ecosystem. Palynological and lithological indicators describe a more progressive evolution of the terrestrial ecosystem surrounding Lake Yoa. Throughout the last 6000 years, the regional vegetation was dominated by grasses (Poaceae), in association with scattered *Acacia* trees (Fig. 2G). Before 4300 cal yr B.P. the regional landscape was an open grass savannah complemented with modest but indicative populations of tropical (Sudanian) trees (e.g., *Piliostigma*, *Lannea*, and *Fluggea virosa*), which today commonly occur in wooded grasslands and dry forests at least 300 km to the south. Their co-occurrence with ferns (Fig. 2G) suggests that these trees formed streambank communities in temporarily flooded river valleys (wadis). The savannah also included tropical herb species (e.g., *Mitracarpus* and *Spermacoce*). This mid-Holocene pollen assemblage was completed by the mountain shrub *Erica arborea*, now restricted to a few small areas above 2900 m altitude in the Tibesti. Substantial input of *Erica* pollen throughout the period with abundant humid plant indicators may suggest that a river from the Tibesti flowed at least seasonally into Lake Yoa until ~4300 cal yr B.P. Drying of this exotic river may have partly accounted for the negative water balance that terminated the lake's freshwater ecosystem shortly thereafter. The first evidence of ecosystem drying in the Ounianga region, however, is already observed at 5600 cal yr B.P., with increasing *Acacia* and the expansion of plants typifying semidesert environments (e.g., *Boerhavia* and *Tribulus*). The demise of tropical trees, accelerating after 4800 cal yr B.P., was initially compensated by expansion of Sahel-type trees and shrubs (e.g., *Commiphora* and *Balanites*), of which the northern limit today does not extend beyond the Ennedi (Fig. 1C). This Sahelian vegetation component, although substantive, was relatively short-lived, because by ~4300 cal yr B.P. *Commiphora* dwindled to a sporadic occurrence.

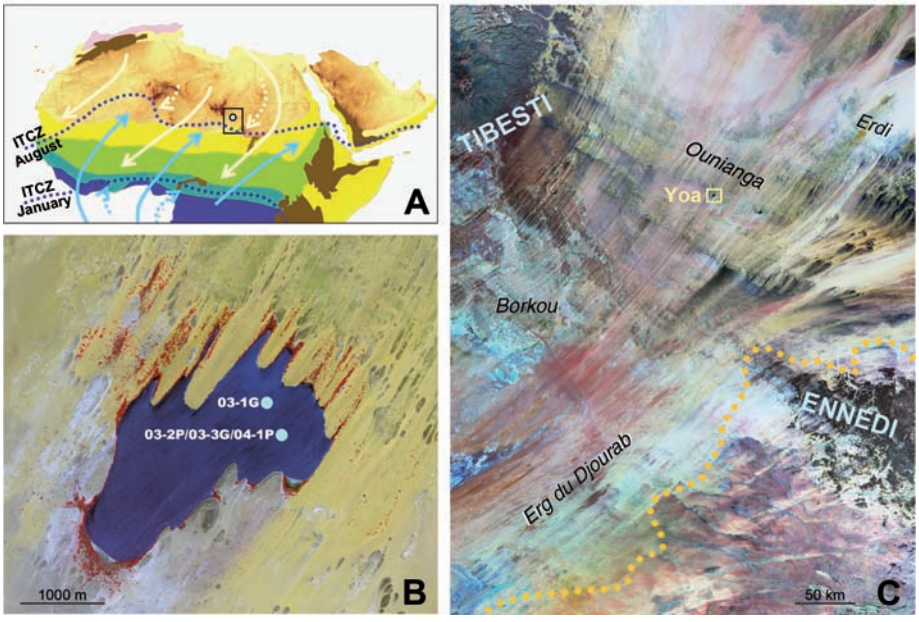

Fig. 1. Location of Lake Yoa [19.03° N, 20.31° E, 380 m above sea level (asl)] at continental and regional scales. (**A**) Map of Africa north of the equator highlighting land >1000 m asl, the natural distribution of vegetation zones (*29*), and synoptic climatology. Arrows: moist tropical Atlantic monsoon circulation (blue) and dry northeasterly trades (light yellow) in relation to the position of the Intertropical Convergence Zone (ITCZ) during Northern Hemisphere summer and winter [adapted from (*9*)]. Vegetation zones, from north to south: Mediterranean evergreen forest (pink), Mediterranean scrubland (light yellow), desert (ochre, with relief), Sahelian wooded grassland (yellow), Sudanian wooded grassland (green), tropical dry forest (blue-green), and tropical rainforest (dark blue); mountain ranges are shown in dark brown. (**B**) Quickbird satellite image of Lake Yoa (4.3 km^2, 26 m deep), bounded to the south and west by sandstone cliffs and to the north and east by dunes of quartz sand. These accumulate in low-wind zones beneath the dissected rim of the Ounianga escarpment, and their progressive migration into the lake has now reached its modern depositional center. *Typha* (cattail) stands develop near groundwater inflow along the northern and eastern lakeshore. Also shown are the locations of sediment cores collected in 2003 and 2004, which together form the studied sediment sequence (*27*). (**C**) Landsat 7 Geocover mosaic satellite image of the Ounianga region showing the main geomorphological features and the northern limit of Sahelian grassland (dotted line) (*28*).

General deterioration of the terrestrial ecosystem of northern Chad ~4800 to 4300 cal yr B.P. is also reflected in a dramatic fall in grass pollen influx, which we interpret to indicate that grass cover became sparse or discontinuous at the landscape scale (despite grass still contributing ~50 to 55% to the pollen sum) (Fig. 2G). This observation is confirmed by the rise in magnetic susceptibility above background values of 2 to 10 $\times 10^{-6}$ SI units from 4300 cal yr B.P., reflecting increased input of wind-blown dust (Fig. 2E) (*27* and SOM text 6). The gradual rise of fine sand (75 to 150 μm) in the upper half of the sequence, above background values of 1 to 5% (Fig. 2F), indicates that from 3700 cal yr B.P. onward, winds also increasingly entrained sand. A first (semi-)desert plant community developed between 3900 and 3100 cal yr B.P. with expansion of herbs such as *Blepharis*, *Boerhavia* (Fig. 2G) and *Tribulus* (scarce), followed at ~2700 cal B.P. by vegetation found today both in the immediate vicinity of Ounianga and throughout the central Sahara (*28*): *Artemisia*, *Cornulaca*, and Amaranthaceae-Chenopodiaceae, with scattered *Salvadora persica* and *Ephedra* trees (Saharan plant taxa, Fig. 2G), as well as *Acacia*.

The near-synchronous immigration of true desert plant types at ~2700 cal yr B.P. is associated with a marked increase in the influx of grass pollen (Fig. 2G), despite our inference of a by now mostly barren desert landscape (SOM text 7). This switch coincides with magnetic susceptibility reaching a plateau value of ~40 $\times 10^{-6}$ SI units, followed by a modest, gradual decline toward the present (Fig. 2E). We interpret this coincidence to reflect the establishment around 2700 cal yr B.P. of the modern regional wind regime, with strong northeasterly trade winds blowing almost year-round (Fig. 1A). In this interpretation, the greater pollen influx mostly reflects enhanced long-distance transport from a now much expanded pollen source area, including scrubland and steppe at the northern fringe of the Sahara. This interpretation is supported by the occurrence after 2700 cal yr B.P. of pollen from plant species (e.g., *Quercus*) (Fig. 2G) that likely originate from the Mediterranean coast (Fig. 1A) (*29*). The expanded pollen source area implies that average northeasterly wind strength must have increased during this time, either because wintertime trade-wind circulation intensified or because a change in the mean position of the Libyan high-pressure cell now channeled low-level northeasterly flow more effectively through the Tibesti-Ennedi corridor. After passing through the Ounianga region, these surface winds continue into the Bodélé depression of the northern Lake Chad basin, the single most important source of Saharan dust (*9*, *30*). Important topographic control by the Tibesti and Ennedi on the generation of erosive Bodélé low-level jet winds (*31*, *32*) implies that our timing of the onset of the modern wind regime in northeastern Chad

has direct bearing on the history of Saharan dust production and export. We interpret the slightly decreasing dust flux (magnetic susceptibility) at Ounianga since 2700 cal yr B.P. to indicate that deflation during the preceding 1500 years had by that time removed all loose soil laid bare through the loss of vegetation cover (SOM text 6). From that moment on, the mineral dust flux became limited by its rate of erosion from dried-out lake basins and exposed bedrock. Redeposition of sand mobilized in this process led to dune development at the foot of the Ounianga escarpment. The rising sand content after 2700 cal yr B.P. (Fig. 2F) may reflect the gradual migration of these dunes into Lake Yoa (Fig. 1B) and their approach of the midlake coring site.

The record of *Typha* (cattail) pollen (Fig. 2G) illustrates the temporal linkages between the evolution of terrestrial and aquatic ecosystems at Ounianga over the past six millennia.

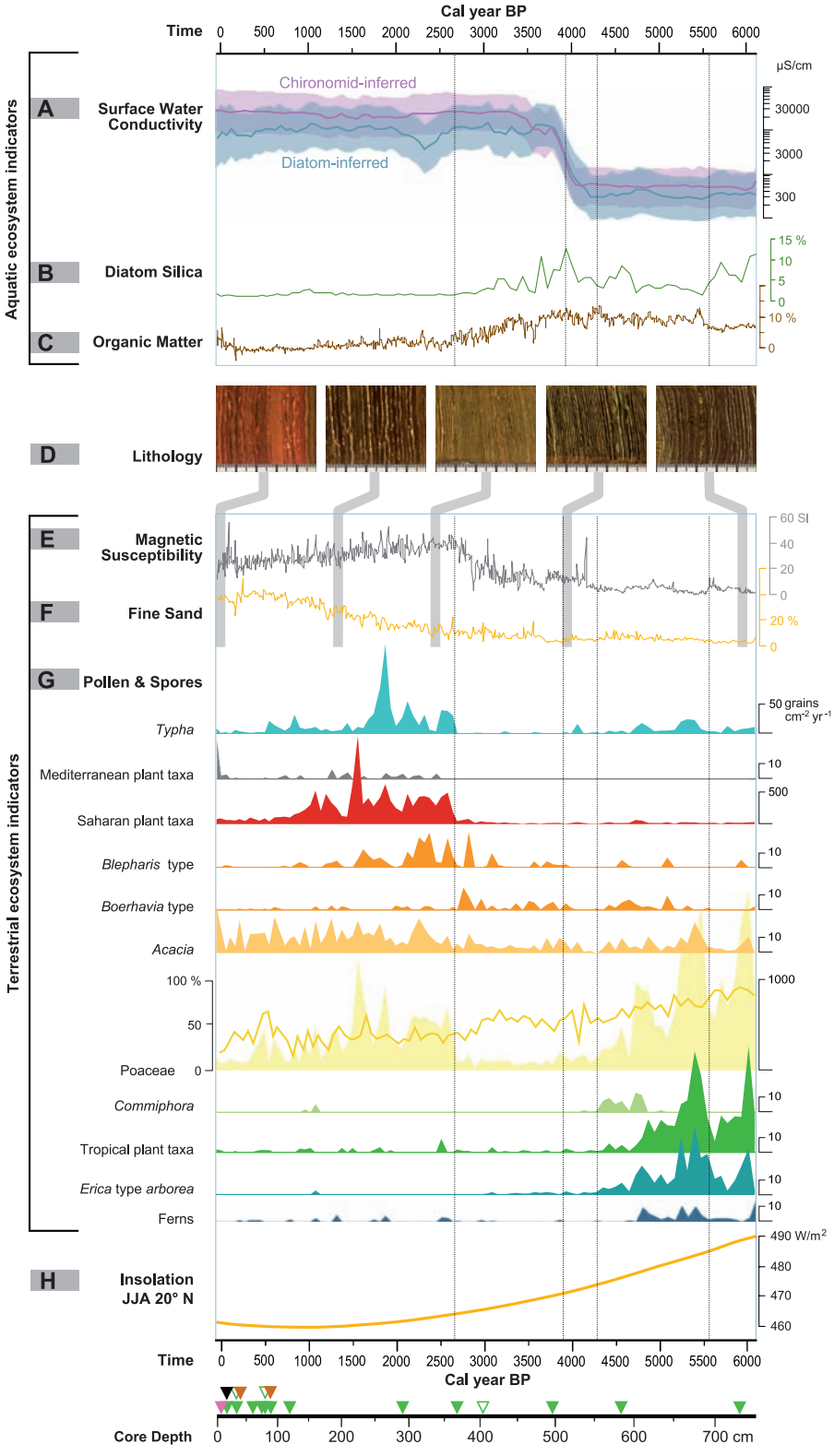

Fig. 2. Evolution of aquatic and terrestrial ecosystem components over the past 6000 years, with episodes of marked change highlighted with stippled vertical lines. The aquatic ecosystem of Lake Yoa is described by paleosalinity reconstructions based on fossil chironomids and diatoms (**A**); and diatom silica in weight percent of SiO_2 (**B**) and bulk organic matter (**C**) as indicators of primary productivity. Core lithology is illustrated by sections of laminated sediment representative for lower, middle, and upper portions of the cored sequence (**D**). The terrestrial ecosystem of the Ounianga region is described by the magnetic susceptibility record of eolian dust input (**E**), the dry-weight fraction of fine sand (**F**), and the influx rate (**G**, right axes) and percentage (G, left axis, Poaceae only) of pollen or spores from principal plant taxa. (**H**) shows local summer insolation over the past 6000 years (*44*). The age-depth model (fig. S1) is constrained by the sediment-water interface (2003 AD), the ^{137}Cs marker of peak nuclear bomb testing (1964 AD, purple) and 17 ^{14}C dates on bulk organic matter (green; open triangles are outliers), with a lake-carbon reservoir correction based on paired ^{14}C dating of bulk organic matter and either charred grass (brown) or 1918 AD in varve years (black) (*27*).

Two episodes of expanded *Typha* swamp occurred at 5500 to 4700 cal yr B.P. and 2700 to 600 cal yr B.P. The first of these coincides with the first recorded evidence for a drying terrestrial ecosystem (Fig. 2G), as well as with indicators of increasing aquatic productivity (Fig. 2C) and community turnover in the phytoplankton (fig. S2). We interpret these data to indicate that by 5600 to 5500 cal yr B.P. climatic deterioration of the regional moisture balance caused parts of the rocky Ounianga plateau to develop drought-tolerant vegetation and forced a lake-level decline that both intensified lake nutrient dynamics and allowed *Typha* swamp to develop along gently sloping shorelines. *Typha* expansion at 2700 cal yr B.P. coincides with the establishment of today's desert plant community and of Lake Yoa as a relatively unproductive, hypersaline desert lake (Fig. 2). We interpret these indicators to signal the stabilization of Lake Yoa at its present elevation, set by the hydrological balance between a hyperarid climate regime, wind-enhanced evaporation, and fossil groundwater input.

Timing and mode of climate change. Arid climatic conditions in the Sahara since ~4300 cal yr B.P. have eradicated all but a few permanent aquatic environments. Paleoenvironmental records covering this period with similar data quality (SOM text 5) are unlikely to exist anywhere else in the arid climate belt of North Africa. Our multiple-indicator reconstruction illustrates the complex relationship between Saharan ecosystems and climate throughout the period of aridification. It gives no indication for abrupt mid-Holocene climate change, or for alternation between marked dry and wet episodes that allowed the vegetation to recover to previous ecological conditions (SOM text 8). Most important, our data do not show an abrupt collapse of the early Holocene terrestrial ecosystem, but a gradual reduction in the abundance of tropical vegetation components followed by loss of grass cover and establishment of the modern desert plant community.

The combined paleoenvironmental evidence indicates that annual rainfall in the Ounianga region was reduced from ~250 mm at 6000 cal yr B.P. to <150 mm by 4300 cal yr B.P., followed by somewhat slower evolution to present-day hyperarid conditions (<50 mm annually) by 2700 cal yr B.P. (SOM text 9). Terrestrial and aquatic ecosystems experienced both gradual evolution and relatively rapid, threshold-type changes, progressing through a predictable sequence of interconnected system responses to climate-driven deterioration of the regional water balance. At the landscape scale this reduction in moisture was effected through decreasing and more intermittent rainfall, lowering of the groundwater table, and the drying out of surface waters. For example, the fairly rapid fresh-to-saline transition of Lake Yoa probably reflects its switch from a hydrologically more open lake system before 4300 cal yr B.P., when substantial surface or subsurface outflow prevented concentration of dissolved salts, to a hydrologically closed system with water output only through evaporation, and a consequent concentration of dissolved salts. The exact timing of this transition depended on a site-specific threshold in the evolving balance between summed inputs (rain, local runoff, groundwater, and river inflow) and outputs (evaporation and subsurface outflow), rather than the timing and rate of regional climate change. Plant community response to climate is also often nonlinear (*25*, *33*), because it is governed by the physiological tolerance of key species to water scarcity and/or osmotic stress (e.g., *34*), by soil moisture thresholds for vegetation persistence, or by the role of vegetation and its spatial patterning in promoting infiltration (*35*) and preventing soil erosion or nutrient loss (*36*, *37*). If mid-Holocene climate change had been concentrated in a relatively short period, the long process of ecological succession and species turnover between "green" and "desert" Sahara states would not have been recorded or would have collapsed into a time window lasting a few centuries rather than the 2.5 millennia observed in our data.

In summary, the Lake Yoa record supports archaeological (*38*) and geological (*14*) data from the eastern Sahara as well as palynological data from the West African Sahel (*39*, *40*) that the iconic record of Saharan dust deposition in the tropical Atlantic Ocean (*2*) is not representative for landscape history throughout dry northern Africa. It is also consistent with climate modeling output (*20*) showing a mostly gradual mid-Holocene precipitation decline over the eastern Sahara (SOM text 8), in line with monsoon-proxy records from elsewhere (*41*–*43*) that indicate a close link between the hydrological cycle in northern subtropical regions and orbital insolation forcing (Fig. 2I). Disagreement with modeling results indicating abrupt mid-Holocene vegetation collapse (*18*, *20*) suggests that the implicated biogeophysical climate-vegetation feedback may have been relatively weak (*6*) and that nonlinear vegetation response to moisture-balance variability superimposed on the long-term drying trend, although certainly affecting individual species distributions, did not lead to abrupt vegetation collapse at the landscape scale.

References and Notes

1. M. Claussen, V. Gayler, *Glob. Ecol. Biogeogr.* **6**, 369 (1997).
2. P. B. deMenocal *et al.*, *Quat. Sci. Rev.* **19**, 347 (2000).
3. COHMAP Members, *Science* **241**, 1043 (1988).
4. J. E. Kutzbach, Z. Liu, *Science* **278**, 440 (1997).
5. A. Ganopolski, C. Kubatzki, M. Claussen, V. Brovkin, V. Petoukhov, *Science* **280**, 1916 (1998).
6. P. Braconnot *et al.*, *Clim. Past* **3**, 279 (2007).
7. A. S. Goudie, N. J. Middleton, *Earth Sci. Rev.* **56**, 179 (2001).
8. J. M. Prospero, P. J. Lamb, *Science* **302**, 1024 (2003).
9. S. Engelstaedter, I. Tegen, R. Washington, *Earth Sci. Rev.* **79**, 73 (2006).
10. Y. J. Kaufman, D. Tanre, O. Boucher, *Nature* **419**, 215 (2002).
11. E. A. Shinn *et al.*, *Geophys. Res. Lett.* **27**, 3029 (2000).
12. T. D. Jickells *et al.*, *Science* **308**, 67 (2005).
13. I. Koren *et al.*, *Environ. Res. Lett.* **1**, 10.1088/1748-9326/1/1/014005 (2006).
14. P. Hoelzmann *et al.*, in *Past Climate Variability Through Europe and Africa*, R. W. Battarbee, F. Gasse, C. E. Stickley, Eds. (Kluwer, Dordrecht, Netherlands, 2004), pp. 219–256.
15. J. E. Kutzbach, B. L. Otto-Bliesner, *J. Atmos. Sci.* **39**, 1177 (1982).
16. S. Joussaume *et al.*, *Geophys. Res. Lett.* **26**, 859 (1999).
17. V. Brovkin, M. Claussen, V. Petoukhov, A. Ganopolski, *J. Geophys. Res. Atmos.* **103**, 31613 (1998).
18. M. Claussen *et al.*, *Geophys. Res. Lett.* **26**, 2037 (1999).
19. H. Renssen, V. Brovkin, T. Fichefet, H. Goosse, *Quat. Int.* **150**, 95 (2006).
20. Z. Y. Liu *et al.*, *Quat. Sci. Rev* **26**, 1818 (2007).
21. J. Adkins, P. Demenocal, G. Eshel, *Paleoceanography* **21**, PA4203 10.1029/2005PA001200 (2006).
22. R. B. Alley *et al.*, *Science* **299**, 2005 (2003).
23. J. A. Rial *et al.*, *Clim. Change* **65**, 11 (2004).
24. M. Scheffer, S. Carpenter, J. A. Foley, C. Folke, B. Walker, *Nature* **413**, 591 (2001).
25. J. A. Foley, M. T. Coe, M. Scheffer, G. L. Wang, *Ecosystems (N.Y., Print)* **6**, 524 (2003).
26. International Atomic Energy Agency, Report RAF/8/036 (IAEA, Vienna, 2007).
27. Materials and methods are available as supporting material on *Science* Online.
28. R. Capot-Rey, *Mém. Inst. Rech. Sahar.* **5**, 65 (1961).
29. F. White, *The Vegetation of Africa* (UNESCO, Paris, 1983).
30. R. Washington, M. Todd, N. J. Middleton, A. S. Goudie, *Ann. Assoc. Am. Geogr.* **93**, 297 (2003).
31. J. Maley, *Global Planet. Change* **26**, 121 (2000).
32. R. Washington *et al.*, *Geophys. Res. Lett.* **33**, L09401 (2006).
33. M. Maslin, *Science* **306**, 2197 (2004).
34. M. Sankaran *et al.*, *Nature* **438**, 846 (2005).
35. S. C. Dekker, M. Rietkerk, M. F. P. Bierken, *Glob. Change Biol.* **13**, 671 (2007).
36. J. van de Koppel, M. Rietker, F. J. Weissing, *Trends Ecol. Evol.* **12**, 352 (1997).
37. S. Kefi *et al.*, *Nature* **449**, 213 (2007).
38. R. Kuper, S. Kröpelin, *Science* **313**, 803 (2006).
39. U. Salzmann, P. Hoelzmann, I. Morczinek, *Quat. Res.* **58**, 73 (2002).
40. M. P. Waller, F. A. Street-Perrott, H. Wang, *J. Biogeogr.* **34**, 1575 (2007).
41. G. H. Haug, K. A. Hughen, D. M. Sigman, L. C. Peterson, U. Rohl, *Science* **293**, 1304 (2001).
42. D. Fleitmann *et al.*, *Science* **300**, 1737 (2003).
43. Y. J. Wang *et al.*, *Science* **308**, 854 (2005).
44. A. Berger, M. F. Loutre, *Quat. Sci. Rev.* **10**, 297 (1991).

45. This research was sponsored by the Deutsche Forschungsgemeinschaft through SFB 389 (ACACIA), the Research Foundation of Flanders (FWO-Vlaanderen, Belgium) and the Centre National de la Recherche Scientifique (France). We thank B. Mallaye of the Centre National d'Appui à la Recherche of Chad for research permission; U. George for support of test coring in 1999; U. Karstens, A. Noren, A. Alcantara, J. F. Crémer, G. Kabihogo, K. Van Damme, A. Myrbo, and M. Blaauw for assistance with data collection, processing, and analysis; and M. Claussen, D. Fleitmann, H. Goosse, Z. Liu, M. Maslin, J.-B. Stuut, and J. van de Koppel for discussion. Cores were logged and archived at the National Lacustrine Core Repository, University of Minnesota, Minneapolis, USA.

Supporting Online Material

www.sciencemag.org/cgi/content/full/320/5877/765/DC1
Materials and Methods
SOM Text
Figs. S1 to S4
Tables S1 and S2
References

7 January 2008; accepted 20 March 2008
10.1126/science.1154913